Supplementary Information

Chiral hexamers of organically modified polyoxometalates *via* ionic complexation

Weiming Guan, Bao Li and Lixin Wu*

State Key Laboratory of Supramolecular Structure and Materials, College of Chemistry, Jilin University, Changchun 130012, China.

**E-mail: wulx@jlu.edu.cn*

Contents

Materials 2
Measurements 2
Synthesis of organic triol modifications 3
Structure characterizations of precursors 6
UV-Vis/CD spectra 12
Estimation of degree of polymerization by ^{1}H DOSY 13
X-ray crystallographic parameters 14
Analysis of the masked solvents for AS-$MnMo_6$ and AR-$MnMo_6$ crystals 15
Additional crystal structure diagram for AS/AR-$MnMo_6$ 18
Characterization on the influence of different cations 22
Additional crystal structure diagram for AA-$MnMo_6$ 22
Reference 24

Materials

(*R*)/(*S*)-3-Aminobutanoic acid, β-alanine, tris(hydroxymethyl)methyl aminomethane, and 1-ethyl-3-(3-dimethylaminopropyl)carbodiimide hydrochloride (EDC·HCl) were purchased from Energy Chemical. Anthracene-9-carboxylic acid and diisopropylethylamine (DIPEA) were purchased from Aladdin Biochemical. 1-Hydroxybenzotriazole (HOBT) was the product from J&K Scientific Chemical. Deuterated reagents for NMR tests were purchased from Cambridge Isotope Laboratories (CIL). HPLC grade solvents were the products from Sigma-Aldrich and Fischer. Spectral grade potassium bromide for FT-IR test was purchased from Sigma-Aldrich. The remaining general chemicals were purchased from Tianjin Fuyu Fine Chemical Company and Sinopharm Chemical Reagent Company. All chemicals were used as received. Ultra-pure water (18.25 MΩ·cm) was used in the experiment.

Measurements

The UV-Vis data were collected on a *Varian CARY 50 Probe* spectrometer with a quartz cell at room temperature. Single Crystal X-ray Diffraction (SCXRD) tests were executed on a *Bruker D8 Venture* diffractometer. The crystals were kept at 100 K during data collection. Graphite-monochromated Mo Kα (λ = 0.71073 Å) X-ray source was selected for the test. ^{1}H NMR results were recorded on a *Bruker AVANCE 500 MHz* spectrometer or *Wuhan Zhongke-Niujin Q. One AS 400 MHz* Instrument. Circular dichroism (CD) spectra were collected on a *Biologic MOS-450/AF-CD* in a 1 mm quartz cell. The results have been smoothed by the Savitzky-Golay method. High-performance liquid chromatography (HPLC) analyses were conducted on a *Shimadzu SPD-20A* liquid chromatography instrument under a UV detector (254 nm) equipped with a *Daicel OD-H* chiral column. Eluent: hexane/isopropanol = 70/30 in v/v. Speed: 1 mL/min. Electron spray ionization mass spectral (ESI-MS) data were performed on an *Agilent1290 - Bruker micrOTOF QII* liquid chromatography-high resolution mass spectrometer combination instrument. Organic elemental analysis data were obtained

on an *Agilent Vario micro cube* element analyzer. TGA results were obtained on a *NETZSCH STA449F3 QMS403D* thermal gravimetric analyzer. Powder X-ray diffraction experiments were conducted on a *Rigaku Smartlab3* instrument. FT-IR data were collected on *Bruker Vertex 80V* Fourier transform infrared spectrometer. ^{1}H DOSY results were recorded on a Bruker AVANCE 500 MHz spectrometer.

Synthesis of organic triol modifications

The anthracene modified triol ligands with *S*-type linker (AS-Tris), *R*-Type linker (AR-Tris) and achiral linker (AA-Tris) were all synthesized as the Fig. S1

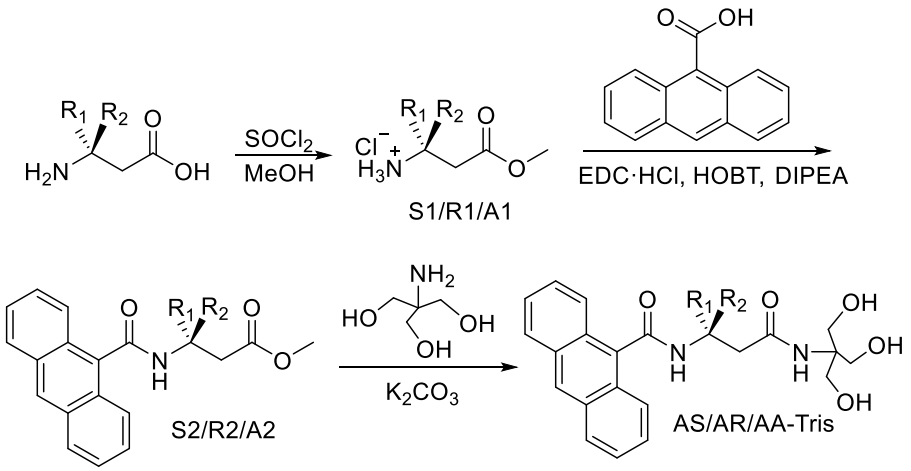

Fig. S1 Synthetic route of AS-Tris, AR-Tris, and AA-Tris.

Synthesis of methyl (S)-3-aminobutanoate hydrochloride (S1). (*S*)-3-aminobutanoic acid (9.70 mmol, 1.00 g) was suspended in 20.0 mL of methanol under stirring. 1.0 mL of thionyl chloride was added dropwise to the suspension. After the solution turned to clear, the solution was heated to reflux for 2 h and then the solvent and excess thionyl chloride were evaporated off to obtain colorless oil as the crude product. The product was used directly for the next step without further purification. ^{1}H NMR (500 MHz,

Chloroform-*d*) δ 8.47 (br, 3H), 3.84 (br, 1H), 3.76 (s, 3H), 2.87 (ddd, *J* = 95.4, 17.0, 5.6 Hz, 2H), 1.53 (d, *J* = 6.4 Hz, 3H).

Synthesis of methyl (R)-3-aminobutanoate hydrochloride (R1). The procedure of **R1** was similar to the route used in **S1** except that (*S*)-3-aminobutanoic acid was replaced by (*R*)-3-aminobutanoic acid. ^{1}H NMR (500 MHz, Chloroform-*d*) δ 8.47 (br, 3H), 3.84 (br, 1H), 3.76 (s, 3H), 2.87 (ddd, *J* = 95.4, 17.0, 5.6 Hz, 2H), 1.53 (d, *J* = 6.4 Hz, 3H).

Synthesis of methyl 3-aminopropanoate hydrochloride (A1). The procedure was similar to the preparation of **S1** except that (*S*)-3-aminobutanoic acid was replaced by β-alanine. ^{1}H NMR (500 MHz, Chloroform-*d*) δ 8.27 (br, 3H), 3.77 (br, 3H), 3.39 (br, 2H), 2.95 (br, 2H).

Synthesis of methyl (S)-3-(anthracene-9-carboxamido)butanoate (S2). Anthracene-9-carboxylic acid (5 mmol, 1.11 g), EDC·HCl (10 mmol, 1.92 g) and HOBT (10 mmol, 1.53 g) were added to 30 mL of dichloromethane under stirring. To the suspension was added 2 g of DIPEA and the solution was stirred for 10 min. Then, **S1** (4.85 mmol, 0.75 g) was added following by the addition of another 1.5 g of DIPEA. The solution was stirred for 15 h at room temperature. The organic phase was separated and washed with water and dried over $MgSO_4$. The final product was purified by column separation (eluent: dichloromethane/methanol = 100/1 in v/v). 0.85 g of product was obtained in yield 54.5%. ^{1}H NMR (500 MHz, Chloroform-*d*) δ 8.50 (s, 1H), 8.08 (dt, *J* = 8.8, 1.1 Hz, 2H), 8.05 – 8.01 (m, 2H), 7.52 (dddd, *J* = 19.5, 7.9, 6.6, 1.3 Hz, 4H), 6.51 (d, *J* = 8.5 Hz, 1H), 4.93 (ddtd, *J* = 12.4, 8.7, 6.8, 5.6 Hz, 1H), 3.73 (s, 3H), 2.87 – 2.75 (m, 2H), 1.51 (d, *J* = 6.8 Hz, 3H). ^{1}H NMR spectrum is shown in Fig. S2.

Synthesis of methyl (R)-3-(anthracene-9-carboxamido)butanoate (R2). The procedure of the preparation of R2 is similar to the route in synthesizing **S2** except that the starting material **S1** was replaced by **R1**. 0.93 g of product was obtained in yield 59.6%. ^{1}H NMR (400 MHz, Chloroform-*d*) δ 8.51 (s, 1H), 8.13 – 8.00 (m, 4H), 7.53 (dqd, *J* = 7.9, 6.6, 1.4 Hz, 4H), 6.55 (d, *J* = 8.6 Hz, 1H), 4.98 – 4.89 (m, 1H), 3.74 (s, 3H), 2.90 – 2.74 (m, 2H), 1.52 (d, *J* = 6.8 Hz, 3H). ^{1}H NMR spectrum is shown in Fig. S3.

Synthesis of methyl 3-(anthracene-9-carboxamido)propanoate (A2). The preparation of **A2** is similar to the route in synthesizing **S2** except that the starting material **S1** was replaced by **A1** and 0.72 g of product was obtained in yield 46.4%. ^{1}H NMR (400 MHz, Chloroform-*d*) δ 8.52 (s, 1H), 8.05 (td, *J* = 6.7, 6.2, 3.4 Hz, 4H), 7.60 – 7.47 (m, 4H), 6.60 (s, 1H), 4.02 (q, *J* = 6.1 Hz, 2H), 3.73 (s, 3H), 2.90 (t, *J* = 6.0 Hz, 2H). ^{1}H NMR spectrum is shown in Fig. S4.

(S)-N-(4-((1,3-dihydroxy-2-(hydroxymethyl)propan-2-yl)amino)-4-oxobutan-2-yl)anthracene-9-carboxamide (AS-Tris). Tris(hydroxymethyl)methyl aminomethane (5 mmol, 0.61 g) and **S2** (2.64 mmol, 0.85 g) were dissolved in 20 mL of dimethyl sulfoxide (DMSO) under sonication. Then K_2CO_3 (10 mmol, 1.38g) was added and the suspension was stirred at room temperature. After the reaction was completed (monitored by TLC, dichloromethane/MeOH = 10/1 in v/v as eluent), the solution was poured into 60 mL of water and stirring for 10 min. The formed precipitate was collected and dried under oven at 60°C as the product in yield 96.9%. Retention time: 8.12 min (Daicel OD-H chiral column, hexane/isopropanol = 70/30 in v/v, 1 mL/min, Fig. S5a). ^{1}H NMR (500 MHz, DMSO-d_6) δ 8.77 (d, *J* = 8.1 Hz, 1H), 8.65 (s, 1H), 8.13 (d, *J* = 8.0 Hz, 2H), 8.06 (s, 1H), 7.95 (d, *J* = 8.1 Hz, 1H), 7.61 – 7.50 (m, 4H), 7.28 (s, 1H), 4.76 (t, *J* = 5.8 Hz, 3H), 4.65 (p, *J* = 7.0 Hz, 1H), 3.59 (qd, *J* = 11.0, 5.9 Hz, 6H), 2.63 – 2.41 (m, 2H), 1.31 (d, *J* = 6.7 Hz, 3H). ^{1}H NMR spectrum is shown in Fig. S6.

(R)-N-(4-((1,3-dihydroxy-2-(hydroxymethyl)propan-2-yl)amino)-4-oxobutan-2-yl)anthracene-9-carboxamide (AR-Tris). The procedure in preparation of **R3** is similar to the one in synthesizing **S3** except that the starting material **S2** was replaced by **R2**. in yield 95.5%. Retention time: 7.18 min (Daicel OD-H chiral column, hexane/isopropanol = 70/30 in v/v, 1 mL/min, Fig. S5a). ^{1}H NMR (400 MHz, DMSO-d_6) δ 8.81 (d, *J* = 8.1 Hz, 1H), 8.66 (s, 1H), 8.14 (d, *J* = 7.7 Hz, 2H), 8.07 (d, *J* = 6.8 Hz, 1H), 7.96 (d, *J* = 8.4 Hz, 1H), 7.58 (t, *J* = 8.4 Hz, 4H), 7.31 (s, 1H), 4.80 (t, *J* = 5.8 Hz, 3H), 4.67 (q, *J* = 7.1 Hz, 1H), 3.60 (qd, *J* = 11.0, 5.9 Hz, 6H), 2.63 – 2.41 (m, 2H), 1.31 (d, *J* = 6.5 Hz, 3H). ^{1}H NMR spectrum is shown in Fig. S7.

N-(3-((1,3-dihydroxy-2-(hydroxymethyl)propan-2-yl)amino)-3-oxopropyl)anthracene-9-carboxamide (AA-Tris). The procedure is similar with the route in synthesizing **S3** except the starting material **S2** was replaced by **A2**. yield 90.3%. ^{1}H NMR (500 MHz, DMSO-d_6) δ 8.84 (t, J = 5.6 Hz, 1H), 8.66 (s, 1H), 8.13 (dd, J = 7.3, 2.7 Hz, 2H), 8.03 – 7.98 (m, 2H), 7.61 – 7.52 (m, 4H), 7.36 (s, 1H), 4.74 (s, 3H), 3.69 (q, J = 6.7 Hz, 2H), 3.59 (s, 6H), 2.64 (t, J = 7.0 Hz, 2H). ^{1}H NMR spectrum is shown in Fig. S8.

Structure characterizations of precursors

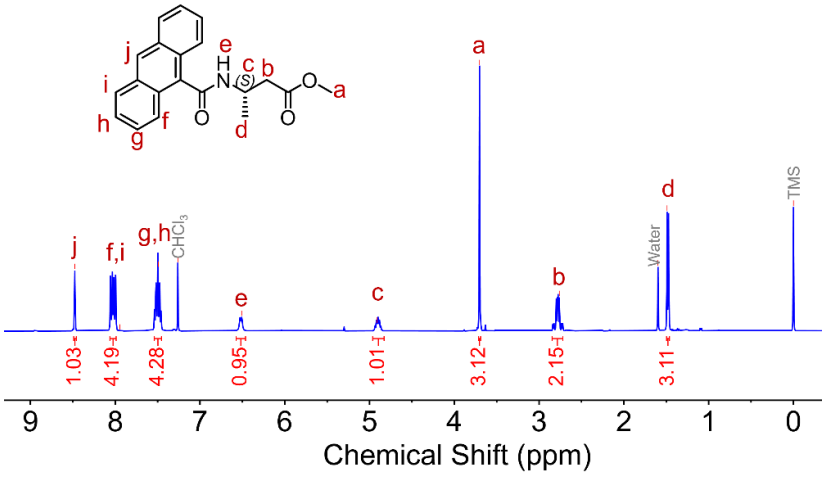

Fig. S2 ^{1}H NMR spectrum (400 MHz) of **S2** in $CDCl_3$.

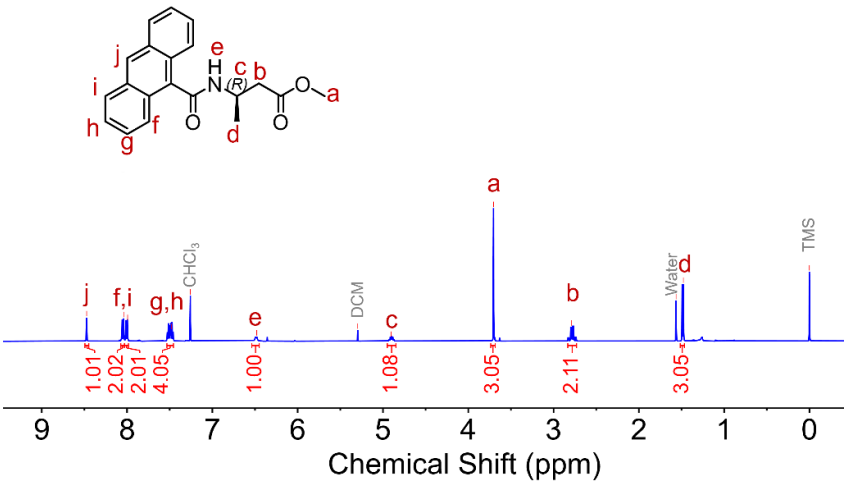

Fig. S3 ^{1}H NMR spectrum (500 MHz) of **R2** in $CDCl_3$.

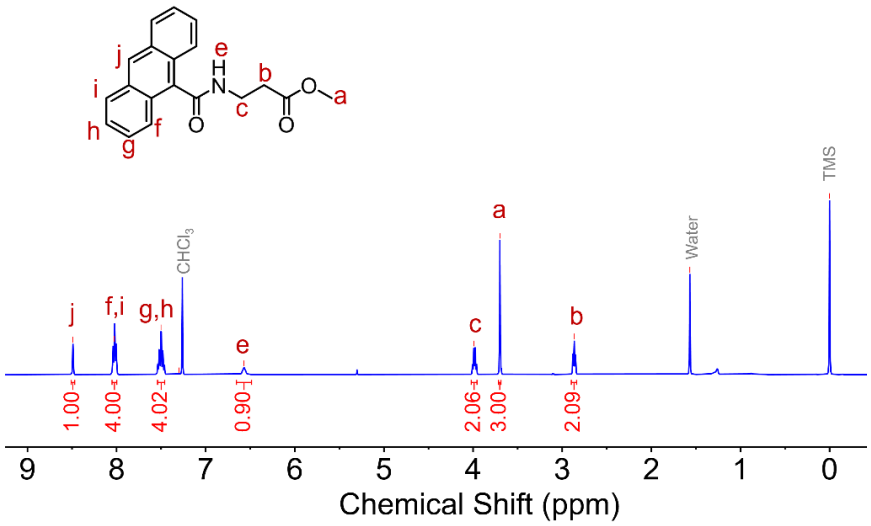

Fig. S4 ^{1}H NMR spectrum (400 MHz) of **A2** in $CDCl_3$.

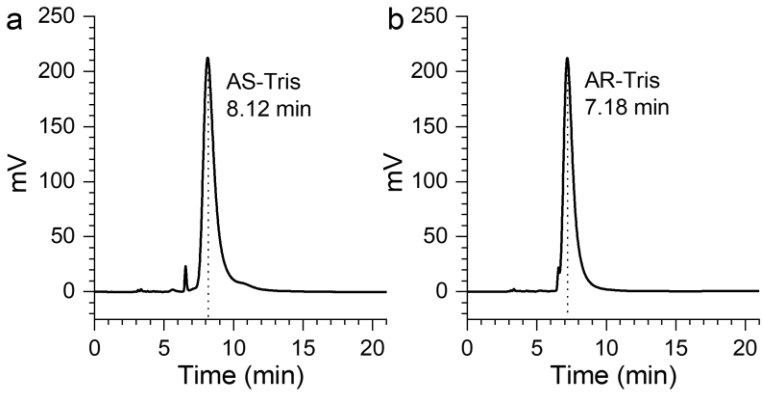

Fig. S5 Chiral HPLC analysis of (a) AS-Tris and (b) AR-Tris over a Daicel OD-H chiral column. Eluent: Hexane/isopropanol = 70/30 in v/v. Speed: 1 mL/min.

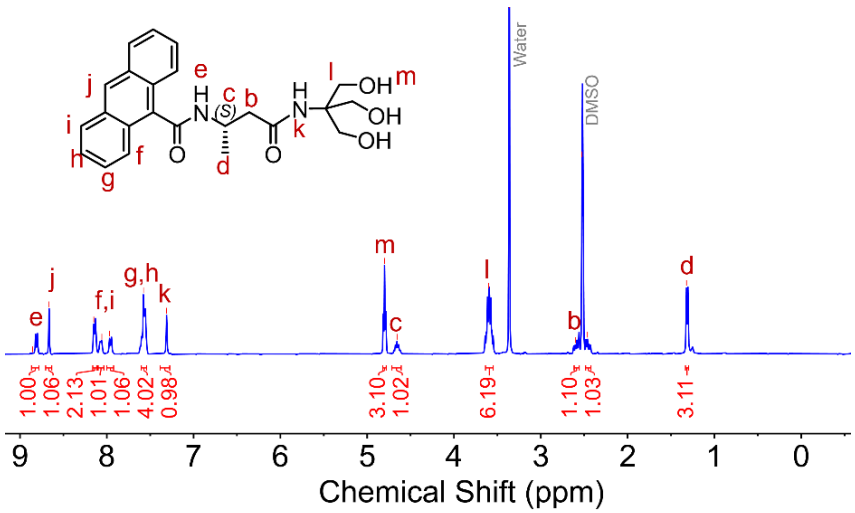

Fig. S6 ^{1}H NMR spectrum (400 MHz) of **AS-Tris** in DMSO-d_6.

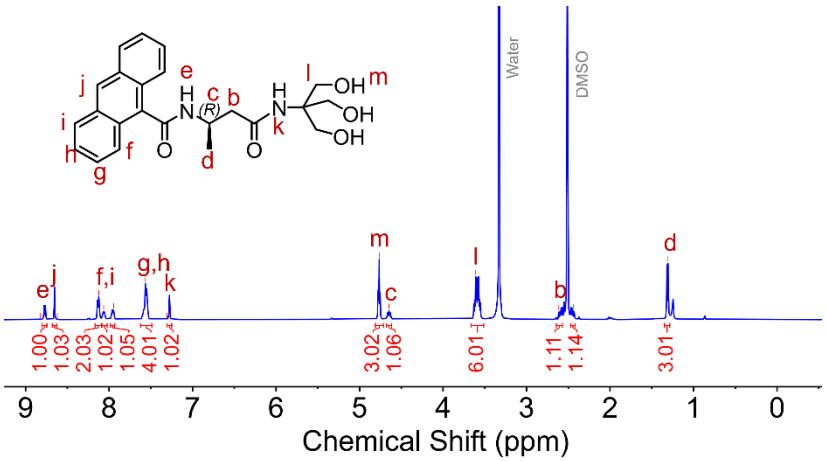

Fig. S7 ^{1}H NMR spectrum (500 MHz) of **AR-Tris** in DMSO-d_6.

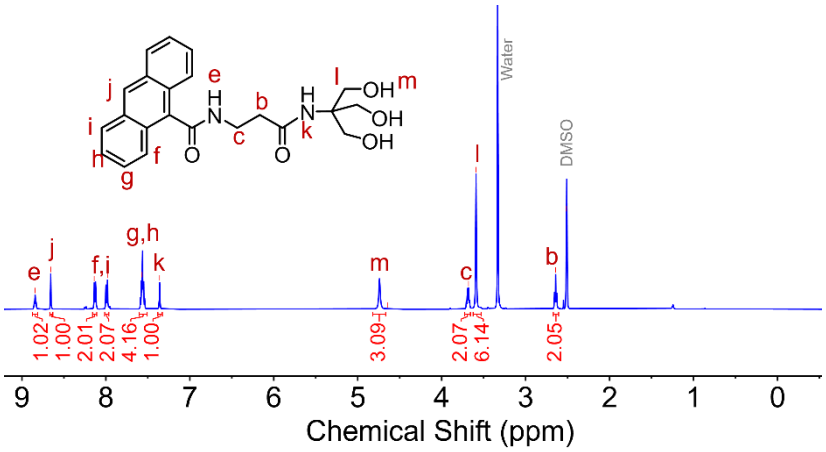

Fig. S8 ^{1}H NMR spectrum (500 MHz) of **AA-Tris** in DMSO-d_6.

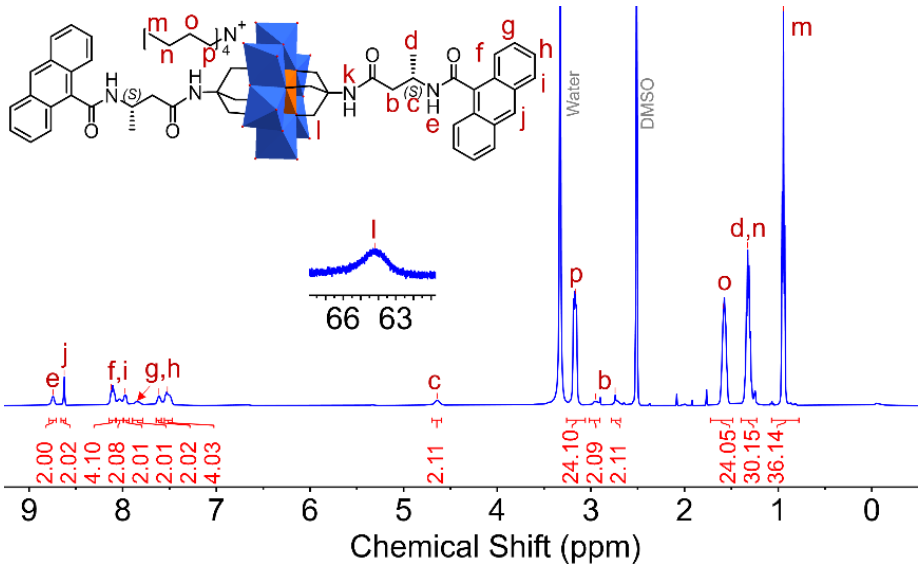

Fig. S9 ^{1}H NMR spectrum (500 MHz) of TBA-AS-MnMo$_6$ in DMSO-d_6.

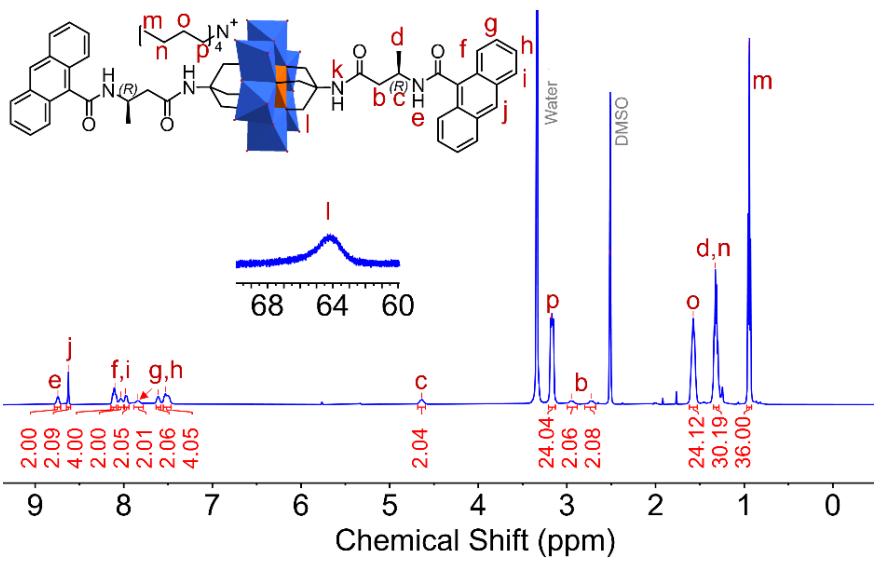

Fig. S10 ^{1}H NMR spectrum (500 MHz) of TBA-AR-MnMo$_6$ in DMSO-d_6.

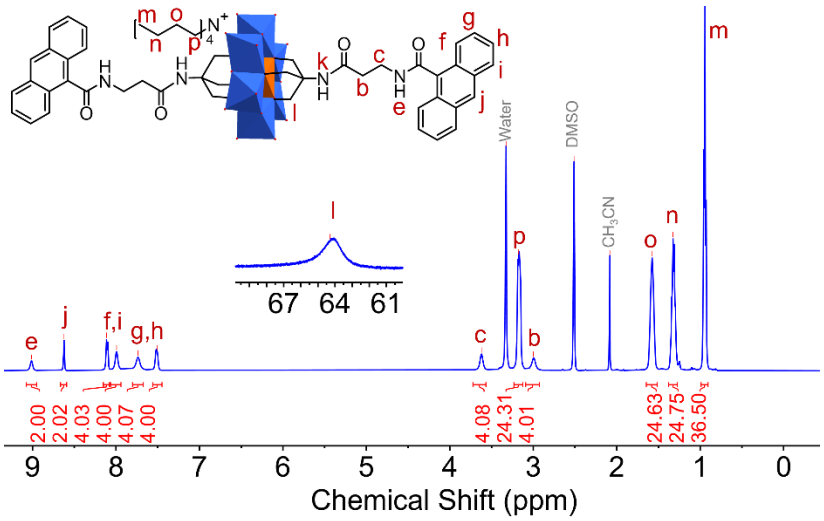

Fig. S11 ^{1}H NMR spectrum (500 MHz) of TBA-AA-MnMo$_6$ in DMSO-d_6.

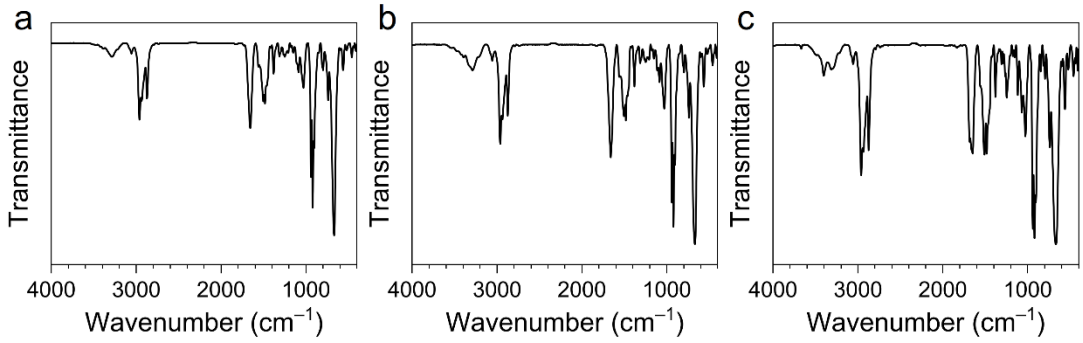

Fig. S12 FT-IR results of (a) TBA-AS-MnMo$_6$, (b) TBA-AR-MnMo$_6$, and (c) TBA-AA-MnMo$_6$

Table S1 Assignments of FT-IR spectra.

TBA-AS-$MnMo_6$ (cm^{-1})	TBA-AR-$MnMo_6$ (cm^{-1})	TBA-AA-$MnMo_6$ (cm^{-1})	Assignments
670	670	670	Mo-O-Mo
903	902	901	Mo=O
920	920	918	Mo=O
940	940	942	Mo=O
1206 – 1264	1206 – 1264	1203 – 1266	Amide C-N stretching vibration
1378 – 1462	1378 – 1462	1378 – 1462	C-H/Aromatic skeleton vibration
1556	1558	1558	Amide N-H deformation vibration
1660	1660	1663	Amide C=O stretching vibration
2871	2872	2869	C-H stretching vibration
2935	2935	2935	C-H stretching vibration
2961	2960	2960	C-H stretching vibration
3057	3057	3057	Anthracene C-H stretching vibration
3212	3212	3215	Amide N-H stretching vibration

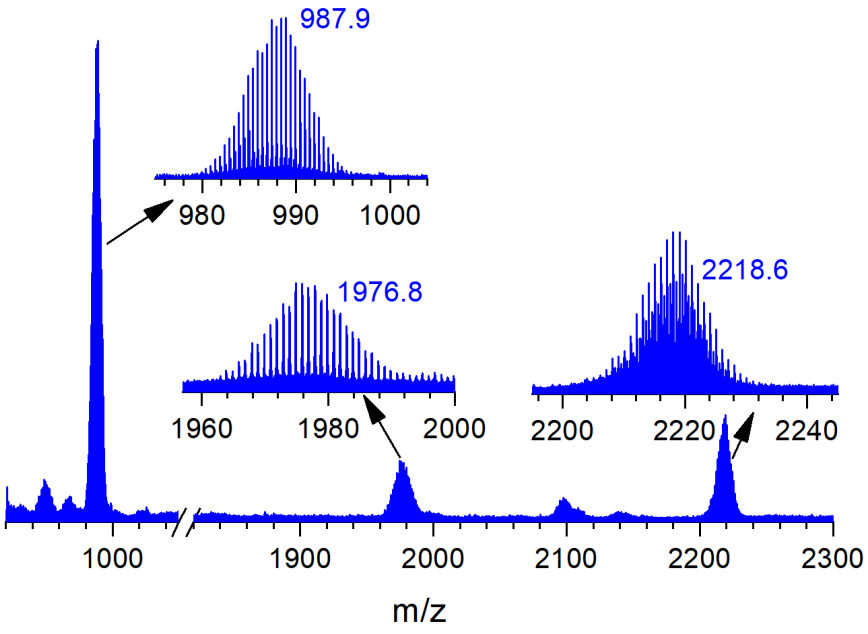

Fig. S13 ESI-MS result of TBA-AS-$MnMo_6$.

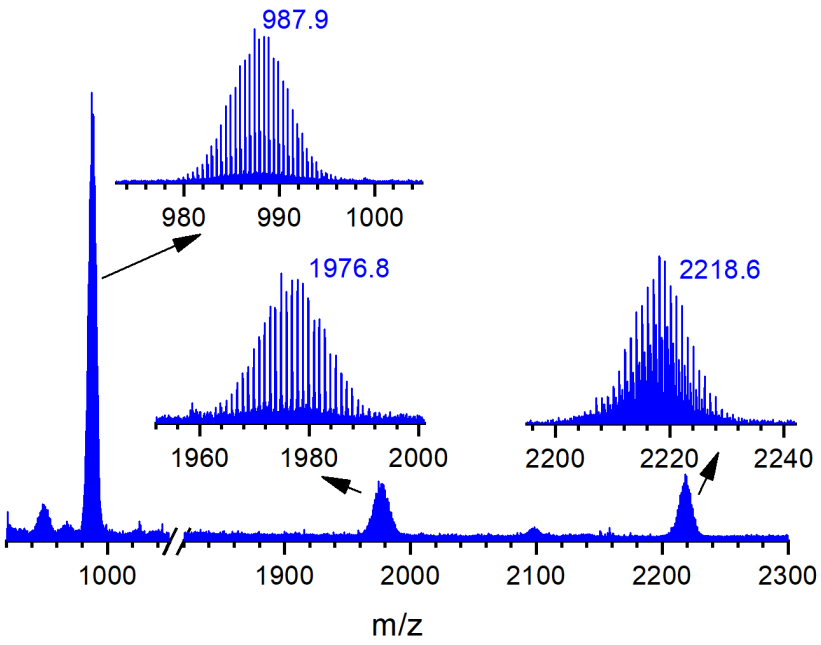

Fig. S14 ESI-MS of TBA-AR-$MnMo_6$.

Table S2 Summary for detailed assignments of the peaks in ESI-MS.

Chemical Formula	Charge	m/z calculated	m/z found
TBA-AS-$MnMo_6$			
$[TBA_2(AS\text{-}MnMo_6)]^-$	1	2218.4	2218.6
$[TBAH(AS\text{-}MnMo_6)]^-$	1	1976.9	1976.8
$[TBA(AS\text{-}MnMo_6)]^{2-}$	2	988.0	987.9
TBA-AR-$MnMo_6$			
$[TBA_2(AR\text{-}MnMo_6)]^-$	1	2218.4	2218.6
$[TBA_3H(AR\text{-}MnMo_6)_2]^{2-}$	2	2097.6	2097.5
$[TBAH(AR\text{-}MnMo_6)]^-$	1	1976.9	1976.8
$[TBA(AR\text{-}MnMo_6)]^{2-}$	2	988.0	987.9

TBA: $[CH_3CH_2CH_2CH_2]_4N^+$.

AR/AS-$MnMo_6$: $[MnMo_6O_{18}[(OCH_2)_3CNHCOCH_2CHCH_3NHCOC_{14}H_9]_2]^{3-}$.

Table S3 Organic elemental analysis.

	N%	C%	H%
TBA-AS-$MnMo_6$: $[(C_4H_9)_4N]_3\{MnMo_6O_{18}[(OCH_2)_3CNHCOCH_2CHCH_3NHCOC_{14}H_9]_2\}$			
Calculated	4.0	45.9	6.3
Found	4.2	45.5	6.3
Error	0.2	0.4	0.0

TBA-AR-MnMo$_6$: $[(C_4H_9)_4N]_3\{MnMo_6O_{18}[(OCH_2)_3CNHCOCH_2CHCH_3NHCOC_{14}H_9]_2\}$			
Calculated	4.0	45.9	6.3
Found	3.8	45.5	6.3
Error	0.2	0.4	0.0
TBA-AA-MnMo$_6$: $[(C_4H_9)_4N]_3\{MnMo_6O_{18}[(OCH_2)_3CNHCOCH_2CH_2NHCOC_{14}H_9]_2\}$			
Calculated	4.0	45.4	6.2
Found	4.2	45.4	6.3
Error	0.2	0.0	0.1

UV-Vis/CD spectra

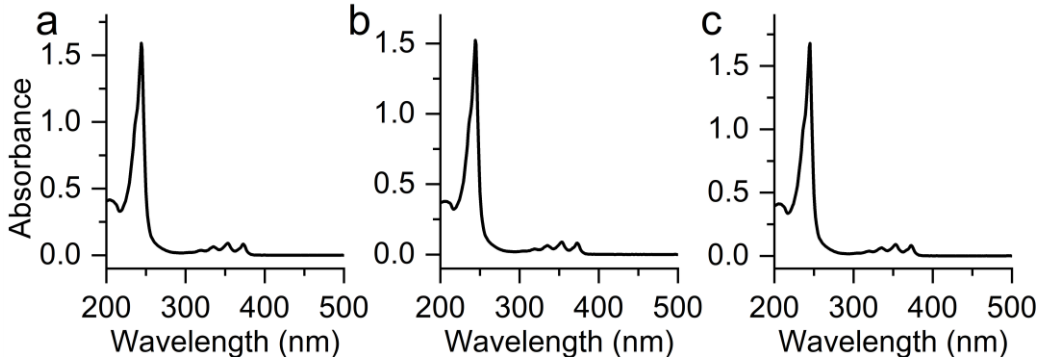

Fig. S15 UV-Vis spectra of (a) TBA-AS-MnMo$_6$, (b) TBA-AR-MnMo$_6$ and (c) TBA-AA-MnMo$_6$ in acetonitrile (0.05 mM) in 1 mm quartz cell.

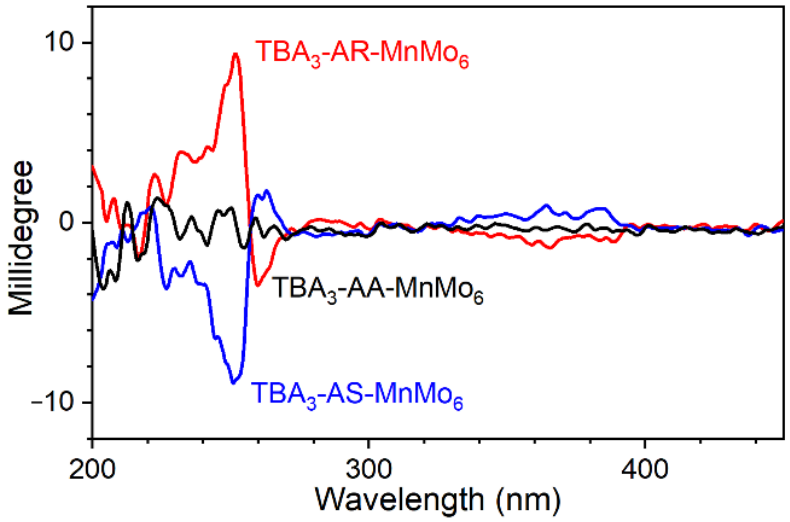

Fig. S16 CD spectra of TBA-AS-MnMo$_6$ (blue line), TBA-AR-MnMo$_6$ (red line), and TBA-AA-MnMo$_6$ (black line) acetonitrile solution (0.1 mM) in 1 mm quartz cell.

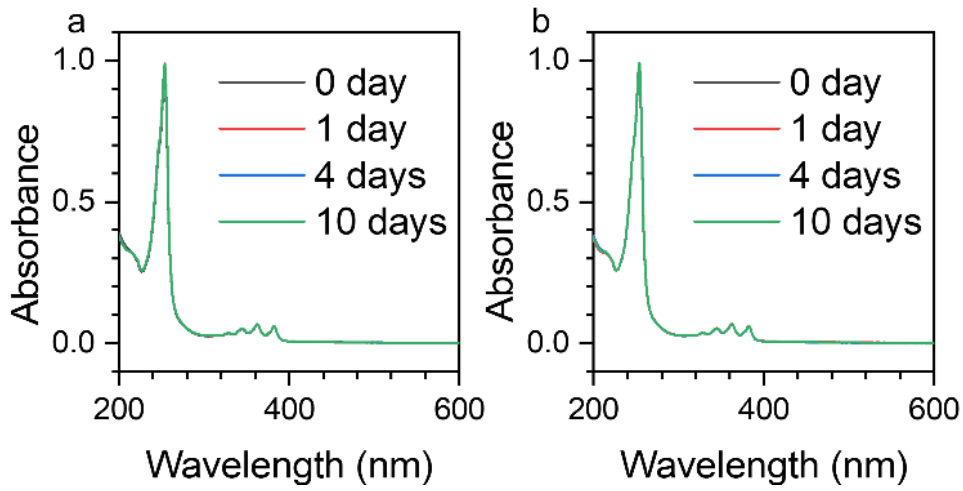

Fig. S17 UV-Vis spectra of TBA-AS-$MnMo_6$ and TBA-AR-$MnMo_6$ in acetonitrile (0.035 mM) in 1 mm quartz cell.

Estimation of degree of polymerization by ^{1}H DOSY

The estimation method refers to the calculation method in the literature.[1] The diffusion coefficients of the anion part of POMs are tested by monitoring the hydrogen on anthracene.

Based on the Stokes-Einstein Equation:

$$D = \frac{kT}{6\pi\eta r_s}$$

k is Boltzmann's constant, T is Kelvin temperature, η is the viscosity of solvent, r_s is thermodynamic radius.

The diffusion coefficient D is proportional to r_s^{-1}. The thermodynamic volume V is proportional to r_s^3. Thus, D^3 is inversely proportional to the thermodynamic volume V.

The degree of polymerization can be seen as the volume ratio of polymer to monomer. So, the average degree of polymerization (DP) can therefore be estimated using the following equation:

$$DP = \left(\frac{D_m}{D_p}\right)^3$$

Where D_m is the diffusion coefficient of the monomer, and D_p is the diffusion coefficient of the oligomer measured by ^{1}H DOSY

For TBA-AS-$MnMo_6$ (Fig. 4a, 4b), after the $NaClO_4$ was added to the solution, the DP can be calculated as:

$$DP = \left(\frac{4.7 \times 10^{-10} m^2/s}{2.6 \times 10^{-10} m^2/s}\right)^3 = 5.9$$

For TBA-AR-$MnMo_6$ (Fig. 4c, 4d) after the $NaClO_4$ was added to the solution, the DP can be calculated as:

$$DP = \left(\frac{4.7 \times 10^{-10} m^2/s}{2.5 \times 10^{-10} m^2/s}\right)^3 = 6.6$$

X-ray crystallographic parameters

Table S4 Crystallographic parameters of AS/AR/AA-$MnMo_6$ crystals.

Name	**AS-$MnMo_6$**	**AR-$MnMo_6$**	**AA-$MnMo_6$**
CCDC No.	2119541	2119542	2119543
Chemical formula	$C_{407.5}ClH_{621.85}Mn_6Mo_{36}N_{81.95}Na_{16}O_{236.9}$	$C_{416.3}ClH_{662.05}Mn_6Mo_{36}N_{86.22}Na_{16}O_{250.36}$	$C_{60}H_{84}MnMo_6N_{10}Na_3O_{36}$
Formula weight	14646.15	15067.54	2220.92
Crystal system	Cubic	Cubic	Triclinic
Space group	$I23$ (No. 197)	$I23$ (No. 197)	$P\bar{1}$ (No. 2)
Unit cell dimensions	a = 30.8142(9) Å b = 30.8142(9) Å c = 30.8142(9) Å α = 90° β = 90° γ = 90°	a = 30.9645(15) Å b = 30.9645(15) Å c = 30.9645(15) Å α = 90° β = 90° γ = 90°	a = 9.3899(9) Å b = 13.0933(13) Å c = 16.5155(16) Å α = 90.088(4) ° β = 95.059(4) ° γ = 99.731(4) °
Volume	29259(3) Å^3	29689(4) Å^3	1993.2(3) Å^3
Z	2	2	1
ρ_{calc}	1.662 g/cm^3	1.686 g/cm^3	1.850 g/cm^3
μ	0.978 mm^{-1}	0.968 mm^{-1}	1.178 mm^{-1}
$F(000)$	14781	15243	1112.0
2θ range	5.288° to 55.016°	4.922° to 51.98°	5.256° to 55.102°

Index ranges	-39 ≤ h ≤ 37 -39 ≤ k ≤ 39 -40 ≤ l ≤ 39	-37 ≤ h ≤ 38 -38 ≤ k ≤ 38 -38 ≤ l ≤ 38	-12 ≤ h ≤ 12 -17 ≤ k ≤ 16 -21 ≤ l ≤ 21
Reflections collected	221521	389367	47040
R_{int}	0.0909	0.1084	0.0764
Data/restraints/parameters	11223/0/455	9741/0/455	8969/72/586
Goodness-of-fit on F^2	1.078	1.159	1.024
R_1[a] [I>=2σ(I)]	0.0392	0.0409	0.0369
R_1[a] (all data)	0.0526	0.0653	0.0602
wR_2[b] [I>=2σ(I)]	0.0949	0.0940	0.0749
wR_2[b] (all data)	0.1049	0.1149	0.0839
Flack parameter	-0.028(10)	-0.028(9)	n/a
Largest diff. peak	0.76 e Å^{-3}	0.91 e Å^{-3}	1.02 e Å^{-3}
Largest diff. hole	-0.76 e Å^{-3}	-0.83 e Å^{-3}	-0.82 e Å^{-3}

[a] $R_1 = \Sigma\,||F_o| - |F_c||/\Sigma|F_o|$. [b] $wR_2 = \Sigma[w(F_o^2 - F_c^2)^2]/\Sigma[w(F_o^2)^2]^{1/2}$.

Analysis of the masked solvents for AS-$MnMo_6$ and AR-$MnMo_6$ crystals

In the process of crystallization, three solvents were used including acetonitrile, DMF and water. So, all three solvents may exist in the solvent accessible void.

For AS-$MnMo_6$:

To figure out the content of DMF and acetonitrile, we redissolved the crystal blocks in DMSO-d_6 and performed an NMR test. The result is shown in Fig. S18.

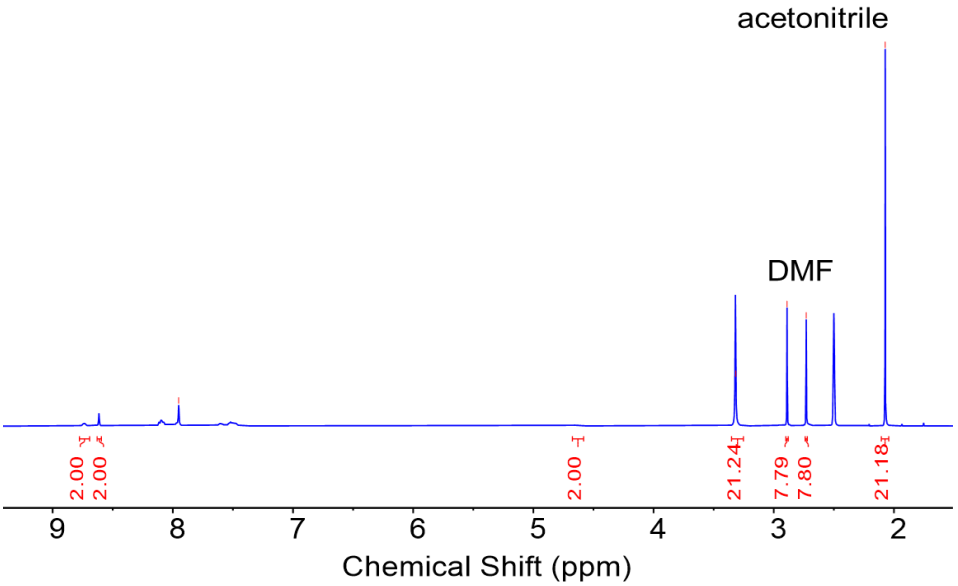

Fig. S18 ^{1}H NMR spectrum of AS-MnMo$_6$ in DMSO-d_6

According to the ratio of NMR integral values, one AS-MnMo$_6$ anion corresponds to 7.06 acetonitrile molecules and 2.6 DMF molecules. Then for a unit cell (including 2 hexamers), it contains 12 AS-MnMo$_6$ anions, 84.72 acetonitrile molecules, 31.2 DMF molecules. In the process of crystal solution, we have resolved 32 acetonitrile molecules with defined structures for one unit cell. So, there are 52.72 acetonitrile molecules and 31.2 DMF molecules are in the solvent accessible void.

The measured number of electrons in the void are 3013 for a unit cell of which 2407 belonged to the acetonitrile and DMF above. The remaining 606 electrons naturally belong to 60.6 water molecules. And this result has been verified by TGA (Fig. S19) and elemental analysis (Table S5).

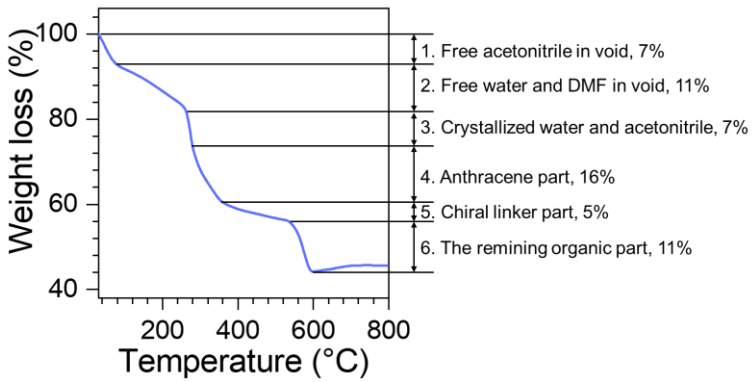

Fig. S19 TGA spectrum of AS-MnMo$_6$ crystal powder under air condition.

Table S5 Elemental analysis result of AS-$MnMo_6$ crystal powder.

	N%	C%	H%
AS-$MnMo_6$ hexamer: $C_{407.5}H_{613.85}N_{82}O_{237}Na_{16}ClMn_6Mo_{36}$			
Calculated	7.8	33.4	4.2
Found	7.4	33.0	4.1
Error	0.4	0.4	0.1

For AR-$MnMo_6$:

According to the ratio of NMR integral values (Fig. S20), by using the same calculation method with AS-$MnMo_6$. The number of acetonitrile molecules in the void is 60.72 and the number of DMF molecules in the void is 31.72. The measured number of electrons in the void are 3474 for a unit cell of which 2605 belonged to the acetonitrile and DMF above. The remaining 869 electrons naturally belong to 87 water molecules. And this result has been verified by TGA (Fig. S21) and elemental analysis (Table S6).

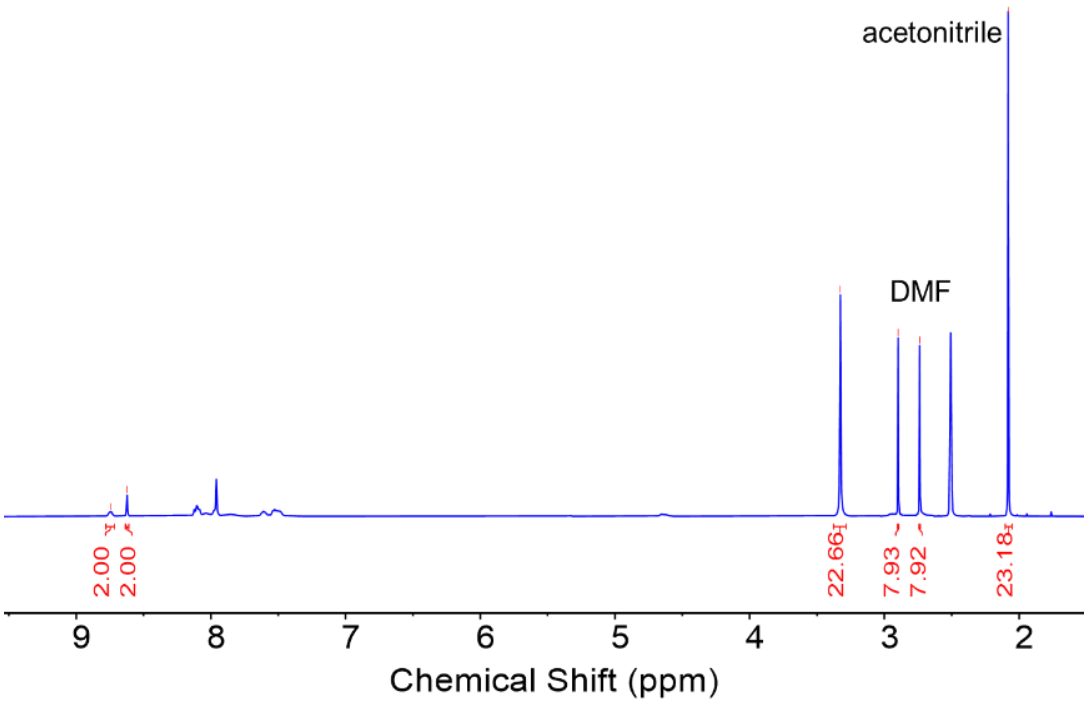

Fig. S20 ^{1}H NMR spectrum of AS-$MnMo_6$ in DMSO-d_6

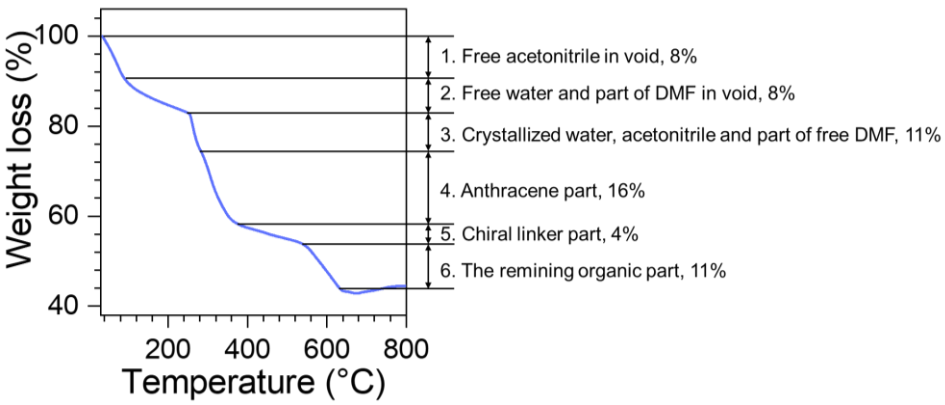

Fig. S21 TGA spectrum of AR-$MnMo_6$ crystal powder under air condition.

Table S6 Elemental analysis result of AR-$MnMo_6$ crystal powder.

	N%	C%	H%
AR-$MnMo_6$ hexamer: $C_{416.3}H_{662.1}N_{86.22}O_{250.36}Na_{16}ClMn_6Mo_{36}$			
Calculated	8.0	33.2	4.4
Found	7.6	32.9	4.3
Error	0.4	0.3	0.1

Additional crystal structure diagram for AS/AR-$MnMo_6$

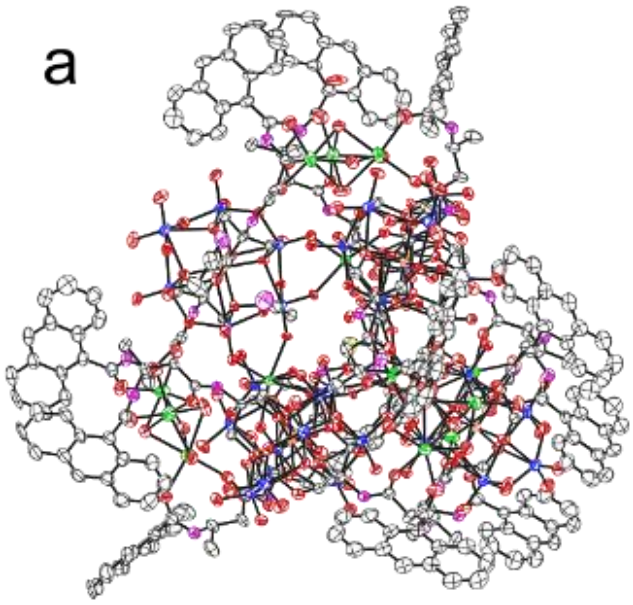

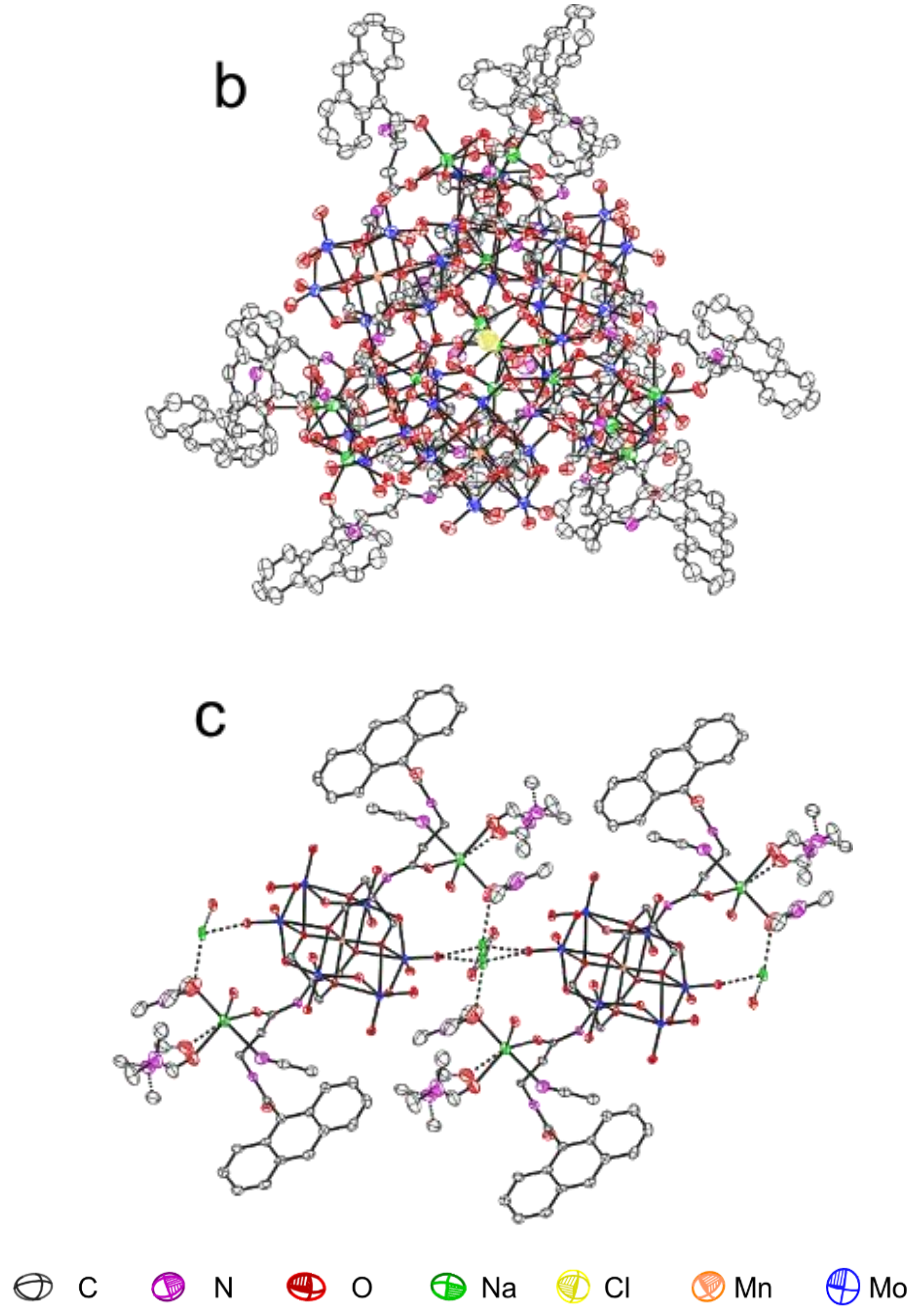

Fig. S22 ORTEP images of the (a) AS-$MnMo_6$ hexamer, (b) AR-$MnMo_6$ hexamer, and (c) AA-$MnMo_6$ polymeric structure as the atoms at 50% probability level (hydrogen atoms are omitted for clarify).

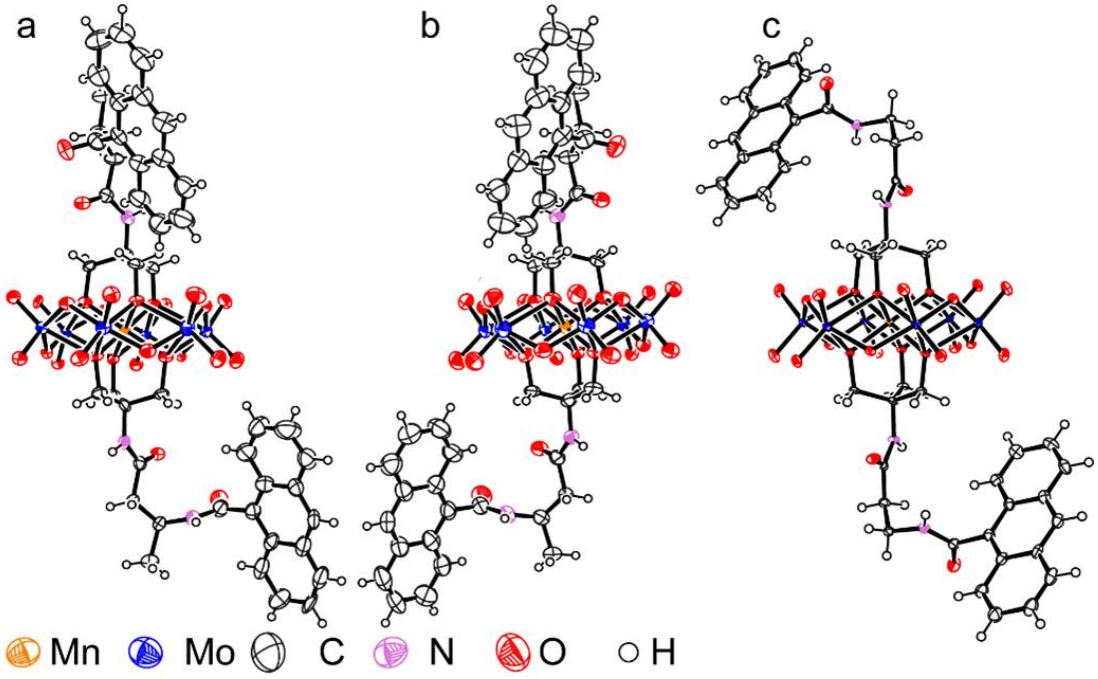

Fig. S23 ORTEP images of the (a) AS-$MnMo_6$, (b) AR-$MnMo_6$, and (c) AA-$MnMo_6$ polyanion monomers as the atoms at 50% probability level.

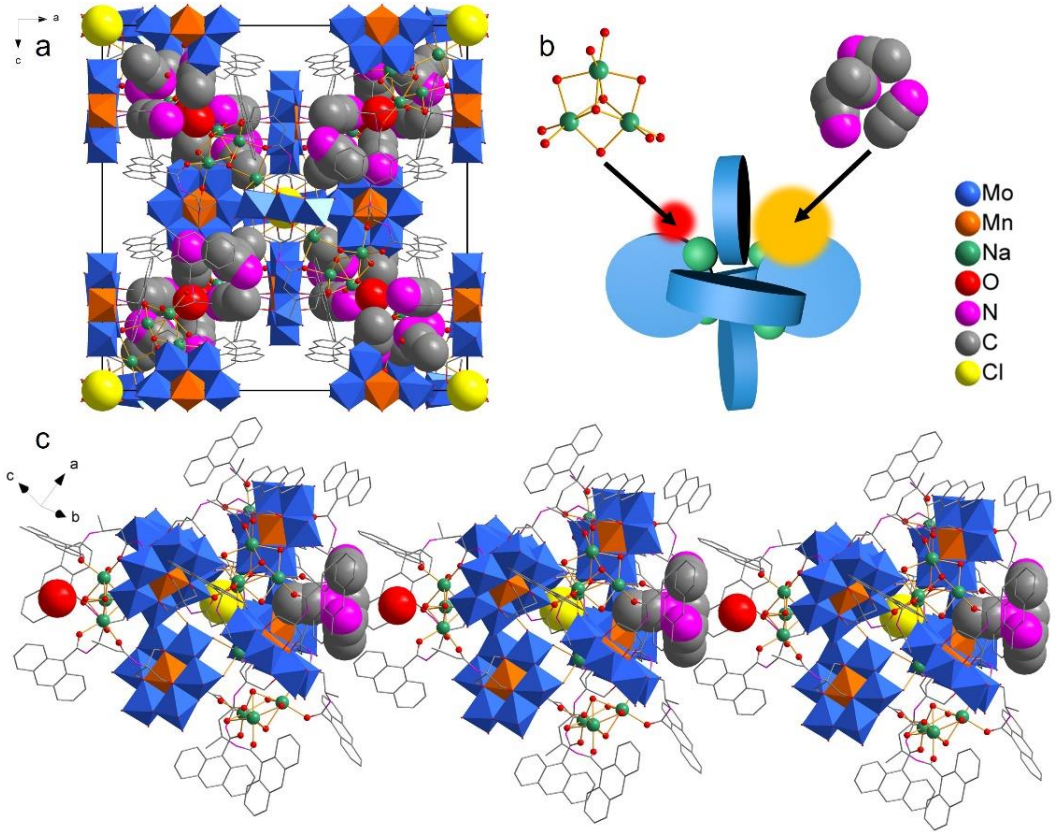

Fig. S24 (a) Cell filling diagram of AS-$MnMo_6$ hexamer, (b) schematic diagram of filling around the AS-$MnMo_6$ hexamer, and (c) packing along the body diagonal of a unit cell.

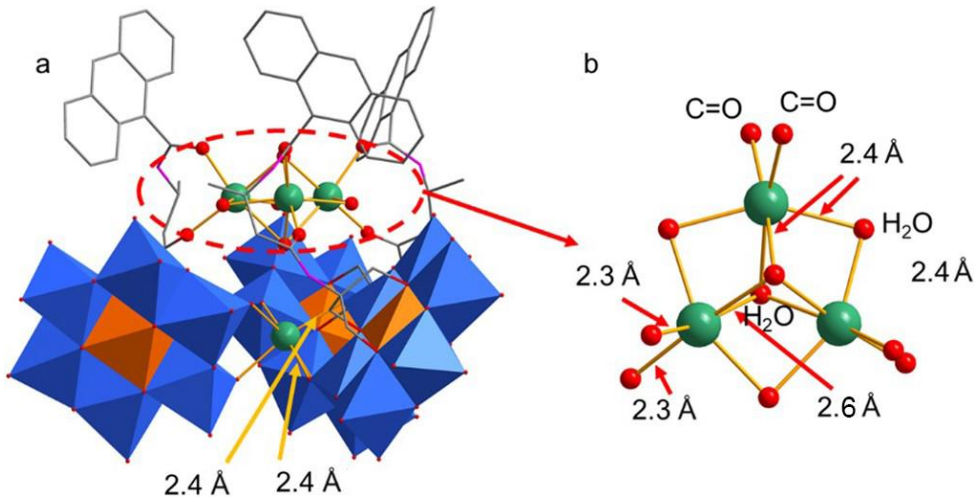

Fig. S25 Coordination position of sodium cations in AR-$MnMo_6$ hexamer and the structure of the Na–O cluster in AR-$MnMo_6$ hexamer.

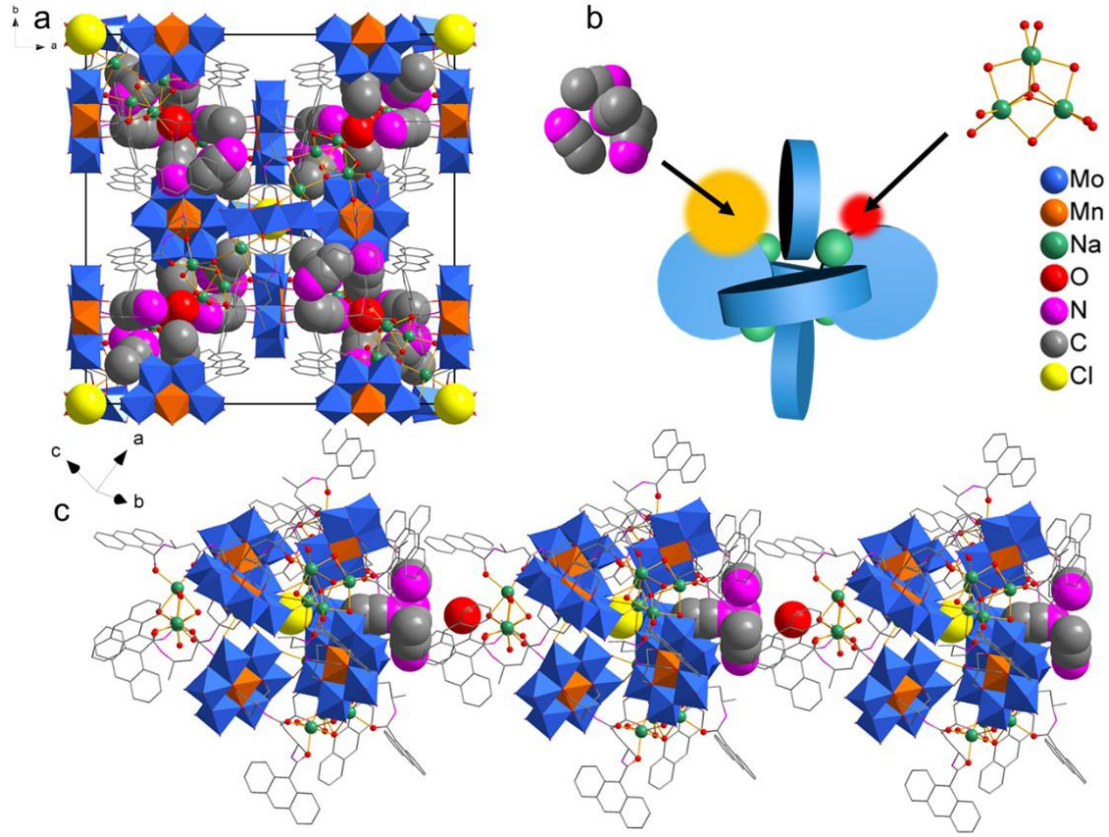

Fig. S26 (a) Cell filling diagram of AR-$MnMo_6$ hexamer, (b) schematic diagram of filling around the AR-$MnMo_6$ hexamer, and (c) packing along the body diagonal of the unit cell.

Characterization on the influence of different cations

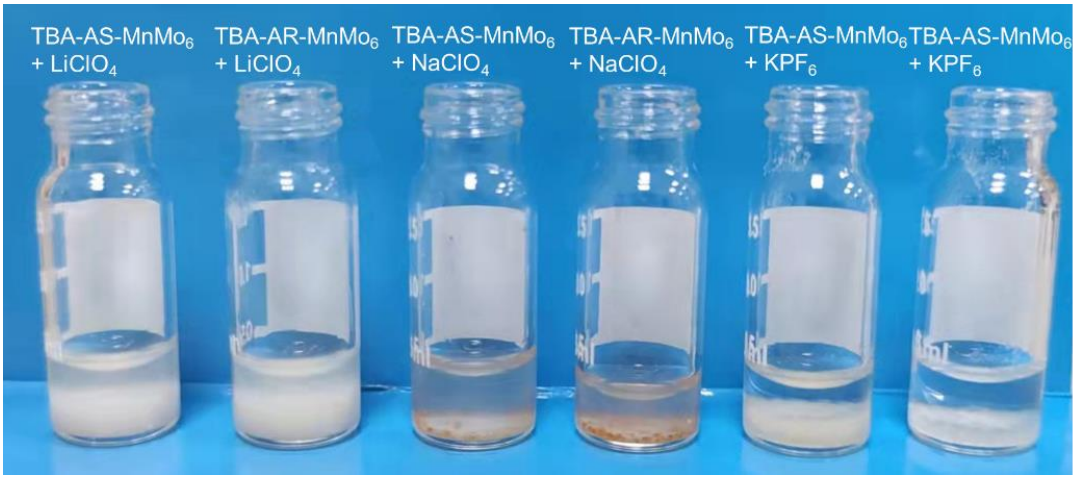

Fig. S27 Digital photograph of the product formed by the assembly between TBA-AS-$MnMo_6$ and TBA-AR-$MnMo_6$ with different cations after diffusion with excess acetonitrile.

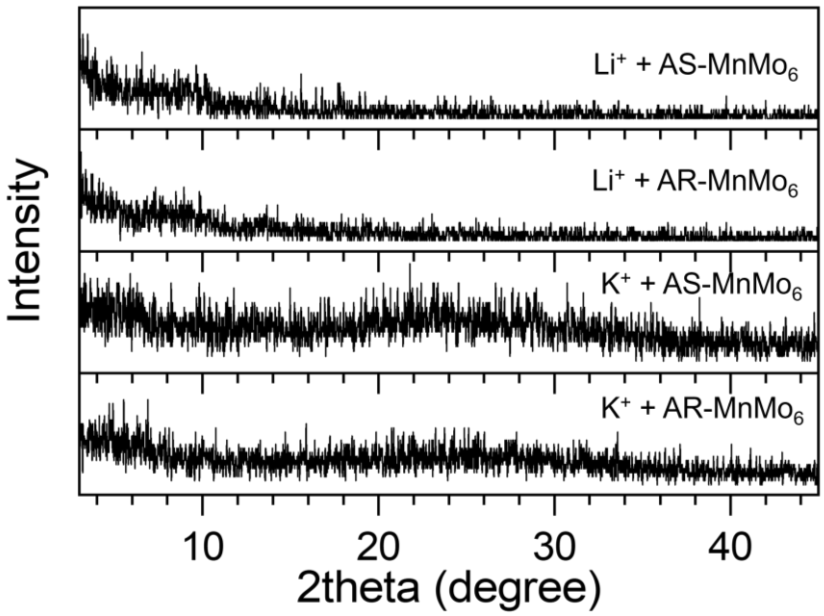

Fig. S28 Powder XRD results of the assemblies between AS-/AR-$MnMo_6$ and Li^+/K^+.

Additional crystal structure diagram for AA-$MnMo_6$

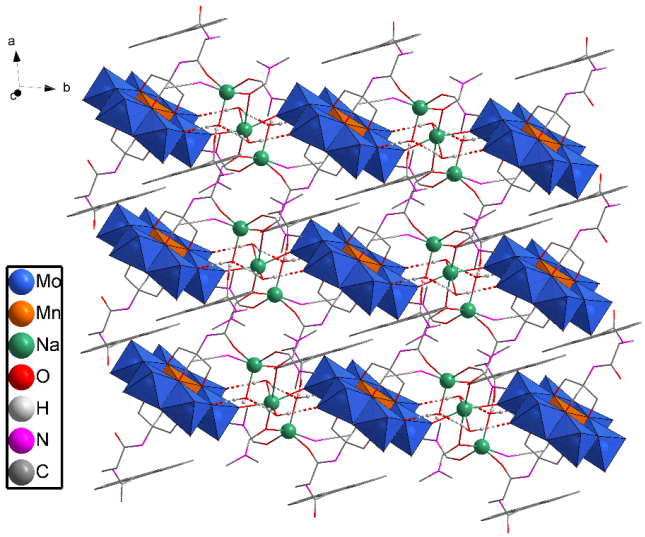

Fig. S29 Packing structure of AA-$MnMo_6$ along crystallographic a-axis by the linkage of hydrogen bonds.

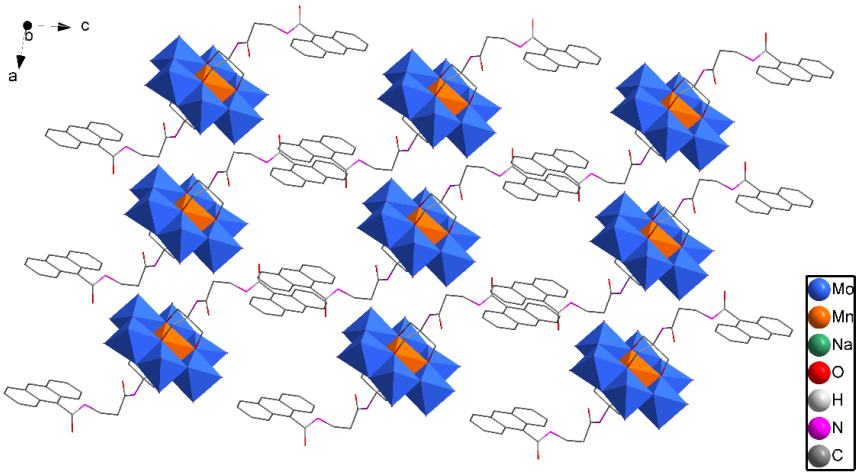

Fig. S30 Packing structure of AA-$MnMo_6$ along crystallographic c-axis showing π-π interaction.

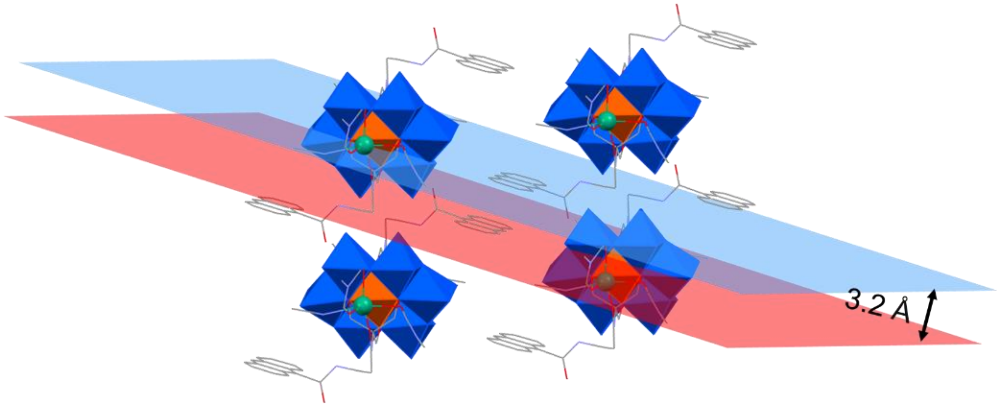

Fig. S31 Interplanar distance measurement of the anthracenes in π-π packing in AA-$MnMo_6$ crystal.

Reference

1. Y. T. Kang, Z. G. Cai, Z. H. Huang, X. Y. Tang, J. F. Xu, X. Zhang, ACS Macro Lett., 2016, 5, 1397–1401.